

# Influence of Operational Conditions on The Drying Kinetics of a Slurry Droplet in A Spray Dryer

Wittaya Julklang and Boris Golman\*

School of Chemical Engineering, Institute of Engineering,  
Suranaree University of Technology, NakhonRatchasima, 30000, Thailand

\*Corresponding author, E-mail: golman@sut.ac.th

Manuscript received October 25, 2012

Revised November 9, 2012

## ABSTRACT

*The effect of operational conditions was studied on the drying kinetics of a slurry droplet in a spray dryer. For this purpose, the mathematical model was developed taking into account the heat and mass transfer resistances inside the droplet. As the result, it was shown that the drying rate of the droplet increases with increasing drying air temperature, air flow rate and slurry concentration, and with decreasing the agglomerate size. It was also confirmed that the heat and mass transfer resistances inside the droplet affect significantly the drying rate.*

**Keywords:** Spray drying, slurry droplet, drying kinetics, drying model.

## 1 INTRODUCTION

The spray-drying process has been used in many industries such as chemical, agricultural, ceramic, food, pharmaceutical, polymer and mineral processing [1]. In comparison with other drying methods, the major advantages of this process are high-energy efficiency, continuous large-scale operation, and flexibility in meeting product requirements.

Recently, many new products were developed using particles produced by spray drying. For instance, nanometer to submicron particles as well as particles of specific morphology were reported to be used for advanced materials due to the large surface area of small particles and special physical and chemical properties derived from their morphology [2]. Mobuset *al.* [3] prepared microparticles for controlled pulmonary delivery of protein via a one-step spray-drying process. Paluchet *al.* [4] crystallized additive-free nanocrystalline microparticles of improved compactibility and compressibility by spray drying of water/

acetone/chlorothiazide mixture. Balgiset *al.* [5] reported on the synthesis of platinum nanoparticles on spherical microflower carbon utilizing spray drying of slurry containing carbon black, polystyrene latex, polyvinyl alcohol and platinum salt. Prepared Pt/C catalyst exhibited superior activity and durability in the high-performance fuel cell applications.

Many operating parameters influence on the drying rate of the slurry feed in the spray dryer. In addition, the range of each parameter varies widely depending on product properties. Therefore, studying the effect of parameters on drying kinetics is important for the design of spray drying equipment and optimization of drying process to produce high-quality agglomerates.

The drying kinetics of a slurry droplet has been investigated both experimentally and theoretically using a mathematical modeling technique. The experimental measurement and the mathematical modeling on drying of single slurry droplet were reported by Nestic and Vonik [6]. However, they used a simplified model neglecting the temperature distribution inside the slurry droplet during drying process. Four operating parameters, such as air temperature and flow rate, droplet size, and slurry concentration, were studied at two different levels. Although the model that includes the temperature distribution inside the droplet was proposed by Farid [7], his model did not take into account the mass transfer in the droplet. Farid [7] studied the same four operating parameters at three various levels.

The distributions of temperature and mass of liquid vapor inside the droplet due to heat and mass transfer resistances were reported by Mezhericheret *al.* [8] and Dalmazet *al.* [9]. Even though Mezhericheret *al.* [8] studied effects of various parameters in wide ranges, his model did not include the temperature distribution inside the droplet during the constant drying rate period. Dalmaz et al. [9] used the assumption of constant

morphology of the droplet during the drying process in developing his model. He studied the effect of common operating parameters at two different levels.

Therefore, there is a need to develop the computational model of drying a slurry droplet including heat and mass transfer resistances in both constant and falling drying rate periods as well as to study the wide range of operational conditions at various levels. The influences of the drying air temperature and flow rate, slurry concentration, initial droplet temperature and diameter are considered in this study on the basis of developed mathematical model.

## 2 THEORETICAL

The mathematical model that includes heat and mass transfer resistances inside the droplet was developed for the analysis of drying kinetics of the slurry droplet. The drying process is separated into two periods, the constant and falling drying rates, as illustrated in Fig. 1.

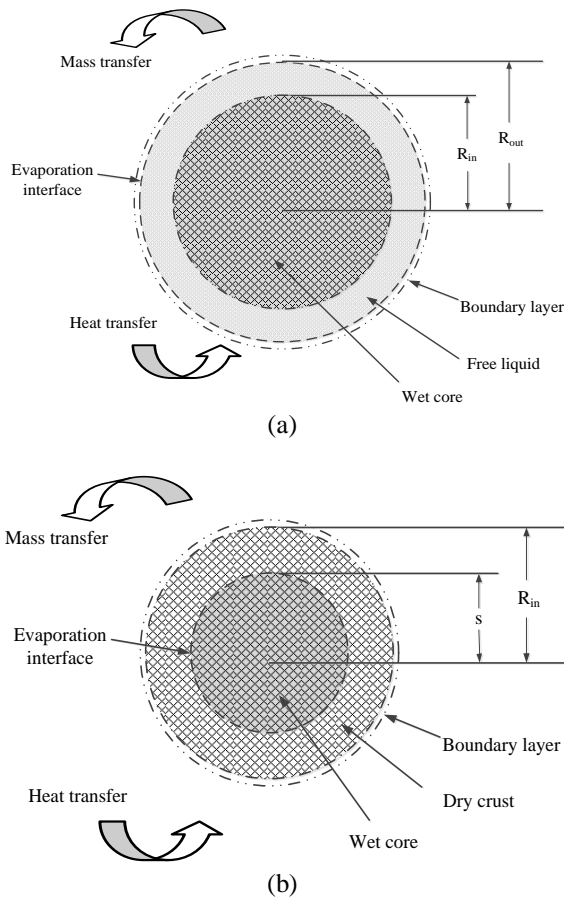


**Fig.1** Model of Slurry Droplet Drying: (a) Constant Rate and (b) Falling Rate Periods.

### 2.1 Mathematical Model of Heat and Mass Transfer inside Droplet

In the constant rate period, the drying droplet is divided into two sections, free liquid and wet core. The droplet generated by atomizer at initial temperature rapidly reaches the wet-bulb temperature. The heat supplied to the droplet surface by convection from the drying air is transferred to the droplet center by conduction. All applied heat in the constant rate period is used for liquid evaporation at the outer surface of the droplet. At the same time, the liquid vapor is transferred from the droplet surface to the drying air by convective mass transfer. The mathematical model of drying kinetics in the constant rate period is shown below.

The temperature distribution in the wet core section of constant porosity,  $\varepsilon$ , is described as

$$\frac{\varepsilon \rho_l C_{p_l} + (1 - \varepsilon) \rho_s C_{p_s}}{k_{co}} \frac{\partial T_{co}}{\partial t} = \frac{\partial^2 T_{co}}{\partial r^2} + \frac{2}{r} \frac{\partial T_{co}}{\partial r} \quad (1)$$

where  $k_{co}$  is the heat conductivity of wet core, and  $\rho_l$ ,  $\rho_s$ ,  $C_{p_l}$  and  $C_{p_s}$  are the densities and heat capacities of liquid and solid phases, respectively.

The temperature distribution in the free liquid section is expressed as

$$\frac{\rho_l C_{p_l}}{k_l} \frac{\partial T_l}{\partial t} = \frac{\partial^2 T_l}{\partial r^2} + \frac{2}{r} \frac{\partial T_l}{\partial r} \quad (2)$$

Where  $k_l$  is the heat conductivity of liquid phase.

The heat balance at the evaporation interface,  $R_{out}$ , is given as

$$\lambda_l \rho_l \frac{\partial R_{out}}{\partial t} = h(T_l - T_{gas}) + k_l \frac{\partial T_l}{\partial r} \quad (3)$$

where  $\lambda_l$  is the latent heat of liquid evaporation,  $h$  is the heat transfer coefficient and  $T_{gas}$  is the temperature of drying air.

The equation for mass transfer at evaporation interface is written as

$$\frac{\rho_l}{M_l} \frac{dR_{out}}{dt} = -k_m (C_{lv} - C_{gas}) \quad (4)$$

where  $k_m$  is the mass transfer coefficient, and  $C_{lv}$  and  $C_{gas}$  are the vapor concentrations at the droplet surface and in the bulk air, respectively.

In the falling rate period, the droplet is also separated into two sections. The first section is called wet core and the temperature distribution in this section is described by the same equation, Eq. (1), as in the constant rate period. The second section is called dry crust. The falling rate period starts when the dry spots appear on the outer surface of droplet, then the evaporation interface moves to the droplet center. The dry crust grows with time leading to increase of heat and mass transfer resistances. The mathematical model of drying kinetics in the falling rate period is shown below.

The temperature distribution in the dry crust is expressed as

$$\frac{(1-\varepsilon)\rho_s C_p s}{k_{cr}} \frac{\partial T_{cr}}{\partial t} = \frac{\partial^2 T_{cr}}{\partial r^2} + \frac{2}{r} \frac{\partial T_{cr}}{\partial r} \quad (5)$$

where  $k_{cr}$  is the heat conductivity of dry crust.

The heat balance on the evaporation interface,  $s$ , is given as

$$\varepsilon \rho_l \lambda_l \frac{ds}{dt} = -k_{cr} \frac{\partial T_{cr}}{\partial r} + k_{co} \frac{\partial T_{co}}{\partial r} \quad (6)$$

The mass balance on the evaporation interface is written as

$$\varepsilon \rho_l \frac{\partial s}{\partial t} = D_{cr} M_l \frac{\partial C_{lv}}{\partial r} \quad (7)$$

where  $D_{cr}$  is the vapor diffusivity in the crust section.

The distribution of liquid vapor concentration,  $C_{lv}$ , in the dry crust section is described as

$$\frac{\varepsilon}{D_{cr}} \frac{\partial C_{lv}}{\partial t} = \frac{\partial^2 C_{lv}}{\partial r^2} + \frac{2}{r} \frac{\partial C_{lv}}{\partial r} \quad (8)$$

The mass transfer from the droplet surface to drying air is expressed as

$$-D_{cr} \frac{dC_{lv}}{dt} = k_m (C_{lv} - C_{gas}) \quad (9)$$

where the effective diffusivity and the heat conductivity in dry crust section are defined as [9]

$$D_{cr} = \frac{2\varepsilon D_{lv}}{3-\varepsilon} \quad (10)$$

$$k_{cr} = \varepsilon k_{lv} + (1-\varepsilon)k_s \quad (11)$$

## 2.2 Mathematical Model of Heat and Mass Transfer outside Droplet

The convective heat and mass transfer coefficients are calculated by utilizing Ranz and Marshall [10] correlations

$$Nu = \frac{h2R_d}{k_g} = 2 + 0.65 Re^{0.5} Pr^{0.33} \quad (12)$$

$$Sh = \frac{k_m 2R_d}{D_{lv}} = 2 + 0.65 Re^{0.5} Sc^{0.33} \quad (13)$$

where  $Nu$ ,  $Sh$ ,  $Re$  and  $Pr$  are the Nusselt, Sherwood, Reynolds and Schmidt numbers for drying air, respectively.

The variations of the average temperature, surface temperature and mass of the droplet, as well as the temperature and liquid vapor concentration profiles in the droplet are calculated by developed model with respect to the drying time.

The ranges of parameters for drying the slurry droplet were selected to cover operating conditions of production processes of advanced particle agglomerates that currently used in industry. The air temperature was varied from 110°C to 350°C, the air flow rate from 0.1 m/s to 2 m/s, the slurry concentration from 25 % to 35% by weight, and the initial droplet temperature from 30°C to 50°C. The porosity of agglomerated product was fixed at 0.5 and the particle diameter was changed from 10 μm to 100 μm. The following parameters were chosen as the standard conditions: air temperature at 200°C, air flow rate at 1 m/s, 30% of slurry concentration, initial droplet temperature at 30°C, and agglomerated product of 50 μm in diameter with porosity of 0.5.

## 3 RESULT AND DISCUSSION

### 3.1 Variation of Air Temperature

To study the effect of air temperature on drying kinetics of the slurry droplet, the air temperature was varied from 110 to 350°C while other operating parameters were set at standard conditions.

The drying time decreased, but the average and surface droplet temperatures increased at high air temperature, as illustrated in Fig. 2. The drying rate

risers with air temperature due to intensification of convective heat transfer and reduction of latent heat of vaporization. The rate of heat transfer from drying air to the droplet surface enhances at higher temperature, as illustrated in Fig. 3 by the higher heat transfer coefficient, resulting in the increase of the surface and average temperatures.

The surface and average droplet temperatures were identical to each other at the beginning and at the end of falling rate period for all air temperatures. However, the surface and average temperatures differed slightly in the middle of the period, as illustrated in Fig. 2. The falling rate period starts with formation of dry spots on the droplet surface while the most part of it is still covered with liquid. Therefore, the surface and average temperatures are similar at the beginning of falling rate period.

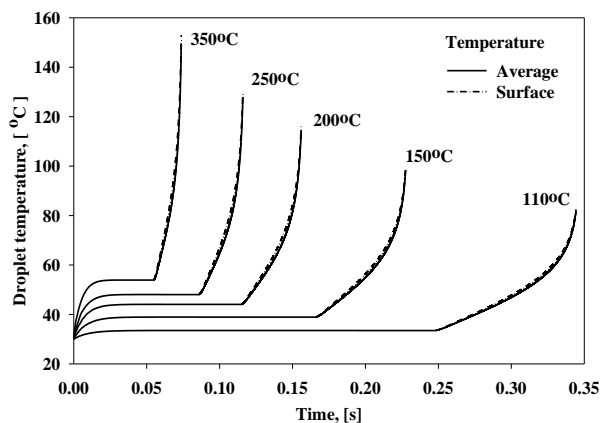


**Fig. 2** Average and Surface Temperatures of the Droplet Dried at Various Air Temperatures.

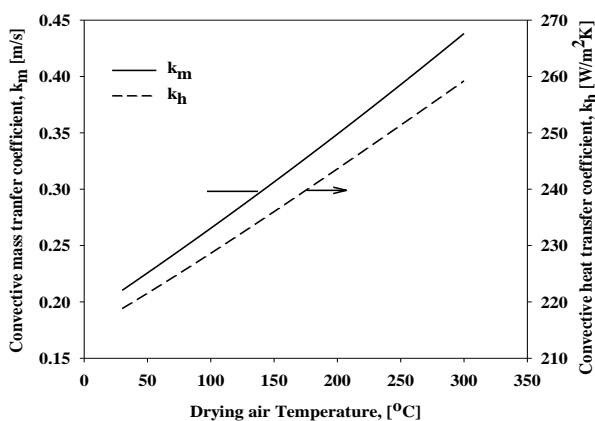


**Fig. 3** Convective Heat and Mass Transfer Coefficients with Drying Air Temperature.

The pressure inside the droplet built up with respect to drying time [8] as liquid vapor concentrated close to the evaporation surface at the outer boundary of wet core, as shown in Fig. 4. This is the result of mass transfer resistance to vapor diffusion in the porous structure of solid crust. Therefore, the wet core becomes significantly hotter for longer drying time, as demonstrated in Fig. 5.

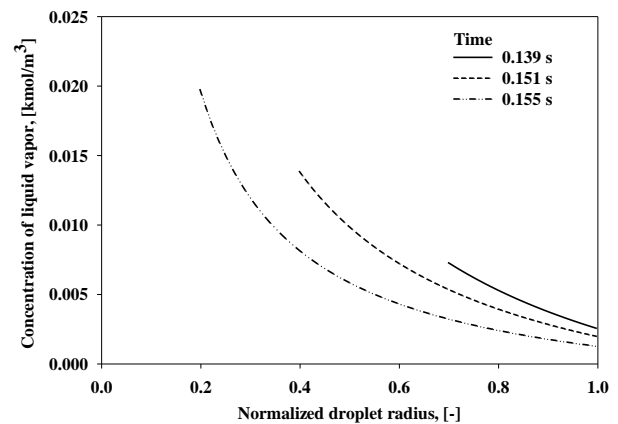


**Fig. 4** Vapor Concentration Profiles inside the Droplet in Falling Rate Period at Air Temperature of 200°C.

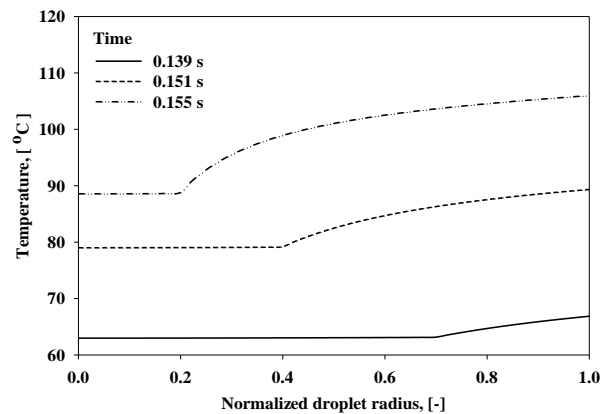


**Fig. 5** Temperature Profiles inside the Droplet in Falling Rate Period at Air Temperature of 200°C.

The enhancement of heat transfer resistance with drying time is illustrated in Fig. 5 by considering the rise of temperature difference between the droplet surface and the evaporation interface. In addition, the temperature profile with convex curvature is observed in the dry crust region of the droplet due to exchange of heat between liquid vapor which diffuses through pore space and the dry crust.

The surface and wet core temperatures increased according to time, yet the size of wet core diminished, as

illustrated in Fig. 5 by comparing the corresponding flat regions. As a result, the difference between surface and average temperatures rose slightly up to the point, which corresponds to the maximum temperature difference. Then the temperature difference reduced until it becomes negligible at the end of drying.

The mass transfer resistance inside the droplet declines as diffusion of liquid vapor enhances at higher drying air temperature. The rate of mass transfer from surface to drying air intensifies with reduction of air humidity. Therefore, the drying rate in the falling rate period rises at higher air temperature as the result of enhanced mass and heat transfer inside the droplet.

Fig. 6 shows the variation of dimensionless droplet weight with respect to time for various air temperatures. The result confirms that the droplet weight reduces more rapidly for higher air temperature because of the higher drying rate at those conditions.

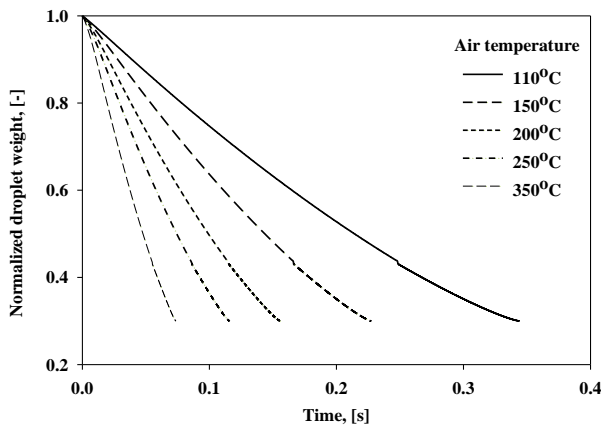


**Fig. 6** Dimensionless Weight of the Droplet Dried at Various Air Temperatures.

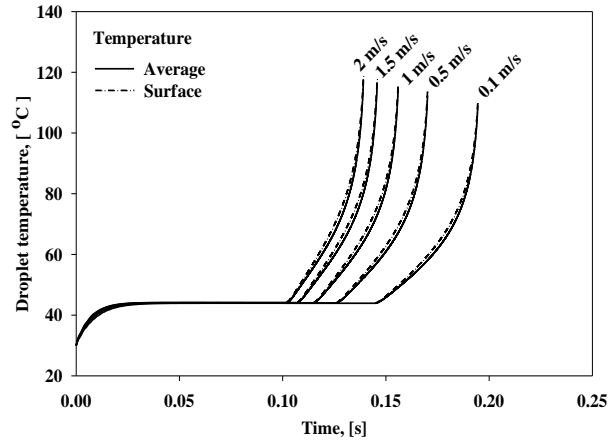
### 3.2 Variation of Air Flow Rate

Fig. 7 indicates the average and surface temperatures of the droplet for various air flow rates. The drying time decreased at higher air flow rate as the boundary layer around the droplet gets thinner. As the result, the external mass and heat transfer resistances decline. Therefore, the rates of heat transfer from drying air to the droplet and mass transfer in opposite direction increase, as shown Fig. 8. This yields to the enhancement of drying rate in the constant rate period.

The rates of mass and heat transfer inside the droplet enhance as the concentration and temperature gradients rise in the falling rate period resulting in higher drying rate.

### 3.3 Variation of Particle Diameter

To study the effect of particle diameter on drying kinetics of the slurry droplet, the particle diameter was varied from 10 to 100  $\mu\text{m}$  corresponding to the initial droplet diameter of 15 to 147  $\mu\text{m}$ .



**Fig. 7** Average and Surface Temperatures of the Droplet Dried at Various Air Flow Rates.

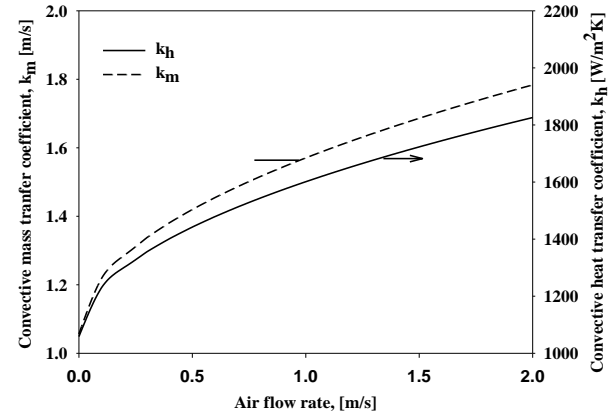
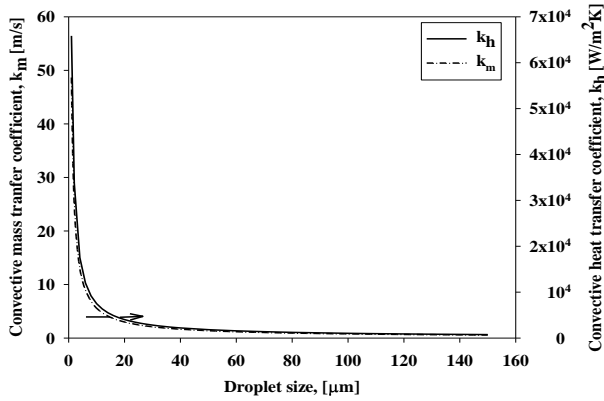


**Fig. 8** Convective Heat and Mass Transfer Coefficients with Air Flow Rate.

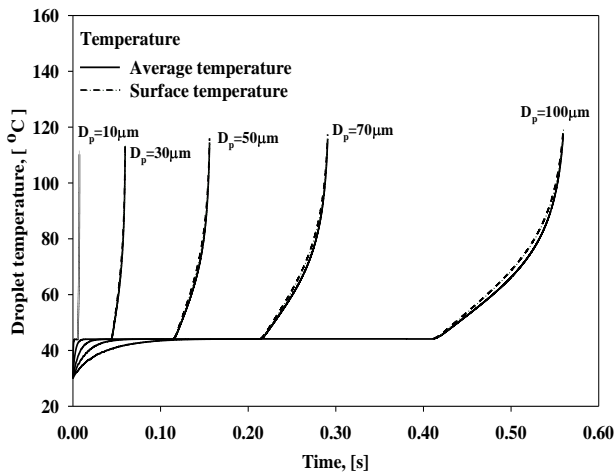
The increase of particle diameter implies the swelling of slurry droplet since the slurry concentration is kept constant. Therefore, the convective heat and mass transfer coefficients reduce by Eqs. (12) and (13), as illustrated in Fig. 9.

Fig. 10 indicates the average and surface temperatures of the droplet for different particle diameters. The drying times in the constant and falling rate periods increased for larger particles due to decline in heat supply to the droplet and mass transfer from the droplet to the drying

air. Therefore, the large particles are dried more slowly than the small ones.



**Fig. 9** Convective Heat and Mass Transfer Coefficients with Droplet Size.



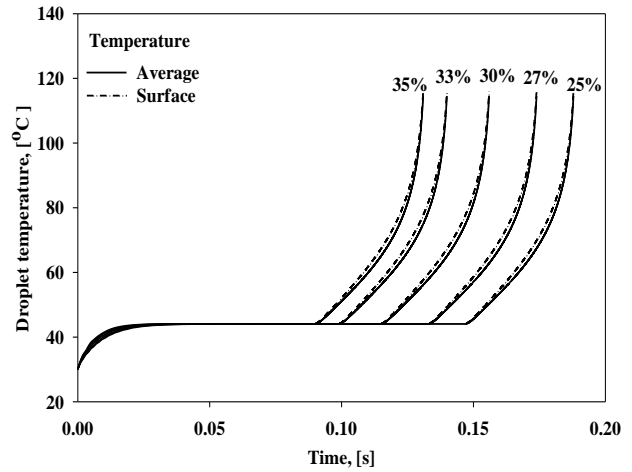
**Fig. 10** Average and Surface Temperatures of the Droplet for Particle of Various Diameters.

**3.4 Variation of Slurry Concentration**

In the present study, the slurry concentration was varied from 25% to 35% w/w. As the porosity and the particle diameter were both fixed, the mass of solid in the slurry was also fixed. The increase of slurry concentration corresponds to the decrease of the amount of liquid in the slurry, yielding to the reduction of free liquid section in the constant rate period. The heat and mass transfer intensify due to the decline in the slurry droplet size, as demonstrated in Fig. 9.

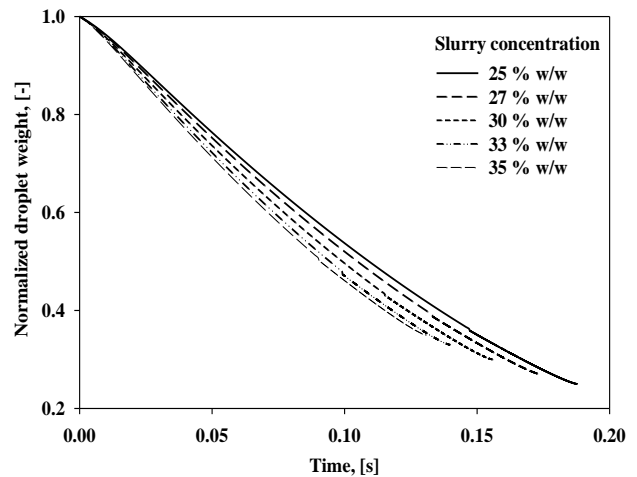
As a result, the drying rate of concentrated slurry was high in the constant rate period, as exemplified in Fig. 11

by variations of average and surface droplet temperatures with drying time.



**Fig. 11** Average and Surface Temperatures of the Droplet Dried at Various Slurry Concentration.

The drying rate in the falling rate period did not change with slurry concentration. The droplet size remains constant after evaporation of free liquid on the droplet surface, leading to the constant external and internal heat and mass transfer resistances.



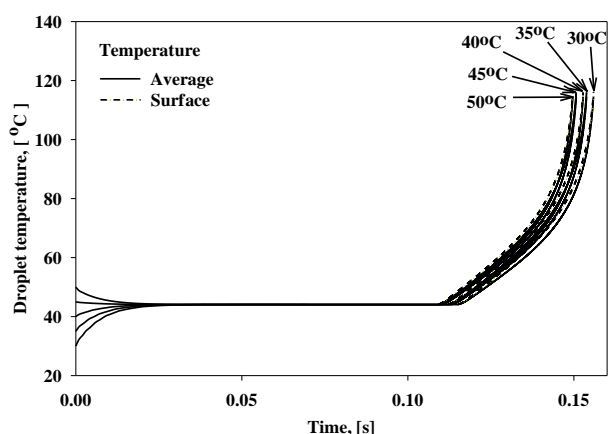
**Fig. 12** Dimensionless Weight of the Droplet Dried at Various Slurry Concentrations.

Fig. 12 shows the variation of dimensionless droplet weight with respect to time. The droplet weight reduced rapidly at higher slurry concentration. In addition, the normalized final weights of particles were not the

same due to the difference in the initial weight of slurry droplets.

### 3.5 Variation of Initial Droplet Temperature

The variations of droplet average and surface temperatures with time are illustrated in Fig. 13 for various initial droplet temperatures. The drying time in the constant rate period declined slightly at high initial droplet temperature due to the evaporation rate enhancement by Eqs. (3) and (4), as a result of high thermal conductivity and low density of liquid. However, the drying rate in the falling rate period did not change with initial droplet temperature as the droplet size, porosity, air temperature and air flow rate were constant in this period.



**Fig. 13** Average and Surface Temperatures of the Droplet Dried at Various Initial Droplet Temperatures.

## 4 CONCLUSION

The effect of various parameters on the drying rate of the slurry droplet in the spray dryer was studied using the developed mathematical model that incorporates the heat and mass transfer resistances inside the droplet.

As the result, it was shown that the drying rate of the droplet increases significantly with increasing drying air temperature, air flow rate and slurry concentration, and with decreasing the agglomerate size. The initial droplet temperature did not have a significant effect on the drying rate.

The wet core temperature increases with the progress of drying during the falling rate period due to the accumulation of liquid vapor inside the droplet. Therefore, it was confirmed that the heat and mass transfer resistances inside the droplet affect significantly the drying rate.

## 5. ACKNOWLEDGMENTS

The authors would like to thank the National Research Council of Thailand for their funding of this research.

## REFERENCES

- [1] K. Masters, *Spray drying handbook*, Longman Scientific and Technical, Harlow, England, 1985.
- [2] A.B.D. Nandiyanto and K. Okuyama, "Progress in developing spray-drying methods for the production of controlled morphology particles: From the nanometer to submicrometer size ranges", *Advanced Powder Technology*, Vol. 22, pp. 1-19, 2011.
- [3] K.Möbus, J.Siepmann and R.Bodmeier, "Zinc-alginate microparticles for controlled pulmonary delivery of proteins prepared by spray-drying", *European Journal of Pharmaceutics and Biopharmaceutics*, Vol. 81, pp. 121-130, 2012.
- [4] K.J. Paluch, L.Tajber, B.Adameczyk, O.I. Corrigan and A.M. Healy, "A novel approach to crystallisation of nanodispersible microparticles by spray drying for improved tabletability", *International Journal of Pharmaceutics*, Vol. 436, pp. 873-876, 2012.
- [5] R. Balgis, G. M. Anilkumar, S. Sago, T. Ogiand K. Okuyama, "Rapid In Situ Synthesis of Spherical MicroflowerPt/C Catalyst Via Spray-drying for High Performance Fuel Cell Application", *Fuel Cells*, Vol. 12, pp. 1615-6854, 2012.
- [6] S. Nestic and J. Vodnik, "Kinetics of droplet evaporation", *Chemical Engineering Science*, Vol. 46, pp. 527-537, 1991.
- [7] M. Farid, "A new approach to modeling of single droplet drying", *Chemical Engineering Science*, vol. 58, pp. 2985-2993, 2003.
- [8] M. Mezhericher, A. Levy and I. Borde, "Heat and mass transfer of single droplet/wet particle drying", *Chemical Engineering Science*, Vol. 63, pp. 12-32, 2008.
- [9] N. Dalmaz, H.O. Ozbelge, A.N. Eraslan and Y.Uludag, "Heat and mass transfer mechanisms in drying of a suspension droplet: a new computational model", *Drying Technology*, vVl. 25, pp. 391-400, 2007.
- [10] W.E. Ranz and W.R. Marshall, "Evaporation from drops", *Chemical Engineering Progress*, Vol. 48, pp. 141-146, 1952.

**Wittaya Julklang**, Biography not availablea at the time of publication.

**Boris Golman**, Biography not availablea at the time of publication.